CMS Physics Analysis Summary

Contact: cms-pag-conveners-susy@cern.ch 2012/04/01

Search for Supersymmetry in Events with Photons and Missing Transverse Energy

The CMS Collaboration

Abstract

We have performed a search for supersymmetry in a gauge-mediation scenario with the gravitino as the lightest supersymmetric particle. The data sample corresponds to an integrated luminosity of 4.7 fb^{-1} of pp collisions at $\sqrt{s} = 7$ TeV, recorded by the CMS experiment at the LHC. We compare the missing transverse energy distribution in events containing either at least two photons plus at least one hadronic jet or at least one photon plus at least two hadronic jets to the spectra expected from standard model processes. No excess of events at high missing transverse energy is observed and upper limits on the signal production cross sections of order 0.01 pb (0.1 pb) at the 95% confidence level for the bino-like (wino-like) scenarios are determined for a range of squark, gluino, and neutralino masses. This analysis is also re-interpreted as a search for Universal Extra Dimensions leading to 95% exclusion values of $1/R < 1335$ GeV for $N_{\text{LEDs}} = 6$.

1 Introduction

Supersymmetry (SUSY), in particular the version based on gauge-mediated SUSY breaking [1–7], is of high theoretical interest for physics beyond the standard model (SM). It stabilizes the mass of the SM Higgs boson, drives the grand unification of forces, and avoids the flavor problems endemic in other SUSY breaking scenarios. Previous searches for gauge-mediated SUSY breaking were performed at ATLAS with 36 pb^{-1} [8] and 1.1 fb^{-1} [9] of pp collision data, CMS with 36 pb^{-1} [10], as well as the Tevatron [11, 12], LEP [13–16], and HERA [17]. The most recent CMS search [18] based on 1.1 fb^{-1} constrained the production of squarks and gluinos to masses above $\sim$ 700-900 GeV based on a simplified model [19]. The other searches put constraints on the gauge boson partners, with the current best lower limit on the neutralino mass [12] of 175 GeV in a general gauge-mediation (GGM) SUSY scenario similar to what is studied here.

In this paper we consider a GGM scenario [20, 21], with the gravitino ($\tilde{\text{G}}$) as the lightest SUSY particle (LSP) and the lightest neutralino ($\tilde{\chi}_1^0$) as the next-to-lightest SUSY particle (NLSP). Long-lived neutralino scenarios (see e.g. Ref. [22]) are not covered in this analysis. The gravitino escapes detection, leading to missing transverse energy ($E_{\text{T}}^{\text{miss}}$) in the event. Assuming that R-parity [23] is conserved, strongly-interacting SUSY particles are pair-produced at the LHC. Their decay chain includes one or several quarks and gluons, as well as a neutralino, which in turn decays to a gravitino and a photon or a Z boson.

We also include the scenario where the NLSP is a pure wino. In that case, the lightest chargino ($\tilde{\chi}_1^{\pm}$) is also a wino, and the chargino-neutralino mass difference is too small for one to decay into the other. In that case the chargino will decay directly into a gravitino and a W boson.

The two topologies studied in this search are:

- two (or more) isolated photons with transverse energy E_{T} above 40 and 25 GeV, at least one hadronic jet, and large $E_{\text{T}}^{\text{miss}}$;
- at least one isolated photon with large E_{T} above 80 GeV, at least two hadronic jets, and large $E_{\text{T}}^{\text{miss}}$.

In neither topology do we veto on the presence of isolated leptons, as especially in the wino co-NLSP case doing so would restrict the acceptance of the neutralino decays into Z and chargino decays into $W^{\pm}$ which could be present for higher neutralino masses. Table 1 gives example decay chains leading to these final states. The table is divided horizontally between single-photon vs di-photon target final states. The vertical direction differentiates between bino NLSP and wino co-NLSP cases. The number of jets produced in the cascades can vary depending on whether gluinos or squarks are produced and the species of quarks in the final state.

Table 1: Some general characteristics of the GGM cascades leading to the topologies of interest.

NLSP type	γ + 2 jets + $E_{\text{T}}^{\text{miss}}$	$\gamma\gamma$ + jet + $E_{\text{T}}^{\text{miss}}$
Bino	$\text{jets} + \tilde{\chi}_1^0\tilde{\chi}_1^0 \to \text{jets} + \gamma + Z + \tilde{\text{G}}\tilde{\text{G}}$	$\text{jets} + \tilde{\chi}_1^0\tilde{\chi}_1^0 \to \text{jets} + \gamma\gamma + \tilde{\text{G}}\tilde{\text{G}}$
Wino	$\text{jets} + \tilde{\chi}_1^0\tilde{\chi}_1^0 \to \text{jets} + \gamma + Z + \tilde{\text{G}}\tilde{\text{G}}$ $\text{jets} + \tilde{\chi}_1^0\tilde{\chi}_1^{\pm} \to \text{jets} + \gamma + W^{\pm} + \tilde{\text{G}}\tilde{\text{G}}$	$\text{jets} + \tilde{\chi}_1^0\tilde{\chi}_1^0 \to \text{jets} + \gamma\gamma + \tilde{\text{G}}\tilde{\text{G}}$

A detailed description of the CMS detector can be found elsewhere [24]. The detector's central feature is a superconducting solenoid providing a 3.8 T axial magnetic field along the beam direction. Charged particle trajectories are measured by a silicon pixel and strip tracker

system, covering $0 \leq \phi \leq 2\pi$ in azimuth and $|\eta| < 2.5$, where the pseudorapidity $\eta = -\ln[\tan\theta/2]$, and θ is the polar angle with respect to the counterclockwise beam direction. A lead-tungstate crystal electromagnetic calorimeter (ECAL) and a brass/scintillator hadron calorimeter (HCAL) surround the tracker volume. For the barrel calorimeter ($|\eta| < 1.479$), the modules are arranged in projective towers. Muons are measured in gas ionization chambers embedded in the steel return yoke of the magnet. The detector is nearly hermetic, allowing for reliable measurement of $E_{\mathrm{T}}^{\mathrm{miss}}$. In the 2011 collision data, unconverted photons with energy greater than 30 GeV are measured within the barrel ECAL with a resolution of better than 1% [25], which is dominated by inter-calibration precision.

2 Data Selection

The data used in this analysis were recorded during the 2011 LHC run and corresponds to an integrated luminosity of 4.7 fb^{-1}. Events were recorded using the CMS two-level trigger system requiring the presence of at least one high-energy photon and significant hadronic activity or at least two photons. This data sample is utilized for the selection of both signal candidates and control samples used for background estimation. The efficiency for signal events to pass the trigger ranges around 40-60% and to satisfy the off-line selection we estimate the efficiency to be above 99% for both analyses. The particular triggers used for the single-photon and di-photon analyses are discussed below.

The photon candidates are reconstructed from clusters of energy in the ECAL. Candidate events are required to have at least one (two) photon(s) with a minimum transverse energy for the single-photon (di-photon) analysis. We require the ECAL cluster shape to be consistent with that expected from a photon, and the energy detected in HCAL behind the photon shower not to exceed 5% of the ECAL energy. To suppress hadronic jets giving rise to photon candidates, we require the latter to be isolated from other activity in the tracker, ECAL and HCAL. A cone of $\Delta R = \sqrt{(\Delta\eta)^2 + (\Delta\phi)^2} = 0.3$ is constructed around the candidates' direction, and the scalar sums of transverse energies of tracks and calorimeter deposits within this ΔR cone are determined, after excluding the contribution from the candidate itself. These isolation sums for the tracker, ECAL and HCAL are added and required to be less than 6 GeV after correcting for pile-up effects.

Photons that fail either the shower shape or track isolation requirement are referred to as *fake photons*. These objects are dominantly electromagnetically fluctuated jets and are used for the background estimation based on data.

The criteria above are efficient for the selection of both electrons and photons. To reliably separate them, we search for hit patterns in the pixel detector consistent with a track from an electron (pixel match). The candidates without pixel match are considered to be photons. Otherwise they are considered to be electrons, which we will use to select control samples for background estimation.

Jets and $E_{\mathrm{T}}^{\mathrm{miss}}$ are reconstructed with a particle-flow technique [26]. This algorithm reconstructs all particles produced in the collision and subsequently identifies them as charged or neutral hadrons, photons, muons, and electrons, by combining information from all detector subsystems. All these particles are clustered into jets using the anti-K_T clustering algorithm with distance parameter of 0.5. To be counted, a jet must have transverse momentum $p_{\mathrm{T}} \geq 30$ GeV, $|\eta| \leq 2.6$ and is required to satisfy the following jet ID requirements. The neutral hadron as well as elecromagnetic fraction of energy contributed to the shower each be < 0.99, that the jet's electromagnetic fraction be $< 0.99\%$ and that the charged hadron fraction be greater than

zero. Jets are corrected for the effects of pile-up to reduce luminosity dependence on jet energies. Events must contain at least one such jet isolated from the photon candidates by $\Delta R \geq 0.5$ for the events to be retained in the signal sample.

3 Background Estimation Methodology

The SUSY signal of interest can be mimicked by SM processes in several ways. The main backgrounds arise from standard model processes with misidentified photons and/or mismeasured $E_{\mathrm{T}}^{\mathrm{miss}}$. The dominant contribution comes from the mis-measurement of $E_{\mathrm{T}}^{\mathrm{miss}}$ in QCD processes such as direct di-photon, photon plus jets, and multijet production, with jets mimicking photons. This background is referred to as background with non-true $E_{\mathrm{T}}^{\mathrm{miss}}$ or as QCD background. The strategy for determining this background is to use control samples that are kinematically similar to the candidate sample while having no true $E_{\mathrm{T}}^{\mathrm{miss}}$.

The second background comes from events with true missing transverse energy. It is dominated by events with a real or fake photon and a W boson that decays into a neutrino and an electron that is mis-identified as a photon. We refer to this sample as background with true $E_{\mathrm{T}}^{\mathrm{miss}}$ or Electroweak (EWK) background. Since all components of this background involve electron-photon misidentification, in order to estimate its contribution to the signal sample, we weight a sample of $e\gamma$ events with $f_{e\to\gamma}/(1-f_{e\to\gamma})$ where $f_{e\to\gamma}$ is the probability to misidentify an electron as a photon. This $e\gamma$ sample has the same requirements imposed on it as the candidate $\gamma\gamma$ sample except a pixel seed is required for one of the EM objects. We also use a sample of ee events where pixel seeds are required on both objects. We measure the p_{T}-dependence of $f_{e\to\gamma}$ by determining the number of $Z \to ee$ events in the ee and $e\gamma$ samples as a function of p_{T}. The overall misidentification rate is $f_{e\to\gamma} = 0.015 \pm 0.002\,(\mathrm{stat.}) \pm 0.005\,(\mathrm{syst.})$ which is used for the di-photon analysis while $f_{e\to\gamma} = 0.008 \pm 0.0025$ for $p_{\mathrm{T}} > 80$ GeV, which is the momentum region relevant for the single-photon analysis and used as misidentification rate in this case.

To study certain SM processes and to generate SUSY signal events, we use the PYTHIA [27] event generator. In particular, we generate SUSY GGM events in a three-dimensional grid of the NLSP, gluino, and squark masses in the benchmark model [19]. Squarks are taken to be mass-degenerate. All other SUSY particles are assumed to be heavy. The production cross-section at NLO QCD is calculated for these points using PROSPINO [28] and is dominated by gluino-gluino, gluino-squark, and squark-squark production. The generated events are then passed through the CMS detector simulation program [29] and reconstructed using the same program as for the collision data so that all features of the detector are included in the signal Monte Carlo acceptances.

4 Di-Photon Analysis

In the following we first describe the results of the di-photon analysis and then discuss the search for GGM SUSY production using single-photon events. The di-photon analysis is based on a di-photon trigger with a threshold of 36 GeV (22 GeV) for the leading (sub-leading) photon. To be in a range of full trigger efficiency, the offline analysis requires at least two photons with $E_{\mathrm{T}} > 40$ GeV (25 GeV) for the the leading (sub-leading) photon in the event.

To estimate the QCD background from data, we utilize two different data sets. The first sample contains two fake photons, in what follows referred to as the fake-fake (ff) sample, comprising QCD multijet events. This is our main dataset to estimate the QCD background. The second data set contains events with two electrons (ee) with the invariant mass between 70 and

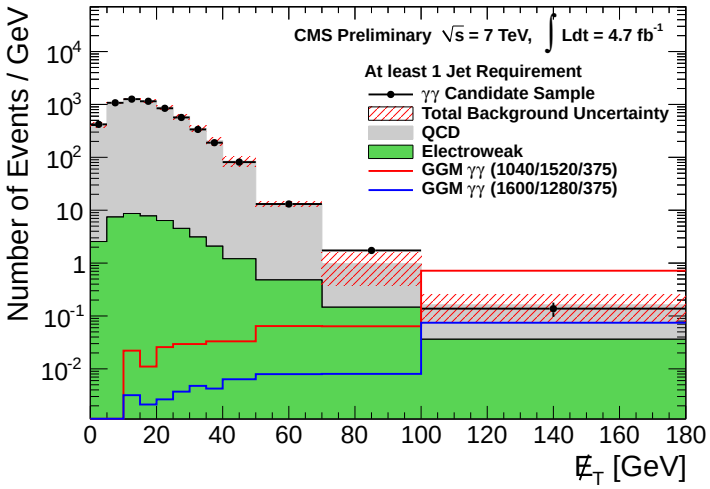

Figure 1: $E_{\mathrm{T}}^{\mathrm{miss}}$ spectrum of $\gamma\gamma$ data compared to QCD prediction together with the small EWK background for events with at least one jet. The red hatched areas indicate the total background uncertainties. Two example GGM points on either side of our exclusion boundary ($m_{\tilde{\mathrm{q}}}/m_{\tilde{\mathrm{g}}}/m_{\tilde{\chi}_1^0}$ in GeV) are also shown.

110 GeV, and is dominated by $Z \to ee$ decays. The ee sample is used to study systematic effects in our background estimate. The E_{T} resolution for electrons and fake photons is similar to the resolution for true photons and is negligible compared with the resolution for hadronic energy, resulting in the $E_{\mathrm{T}}^{\mathrm{miss}}$ resolution being dominated by the latter. The events in both control samples are re-weighted to reproduce the (di-)photon transverse energy distribution in the data, and, therefore, the transverse energy of hadronic recoil against the photon(s). The $E_{\mathrm{T}}^{\mathrm{miss}}$ distributions in the re-weighted control samples show fair agreement within uncertainties. The shape of the ff sample is used to determine the magnitude of the QCD background after normalizing the ff background shape to the di-photon data in the region of low $E_{\mathrm{T}}^{\mathrm{miss}} < 20$ GeV. We choose to use the prediction from the ff sample as main estimator of the QCD background while the difference with the QCD estimate from the sideband subtracted ee sample is chosen to give an estimate of the systematic uncertainty on our determination of the QCD background. As illustration of the validity of the QCD background estimate, in the E_{T} region of 30 to 50 GeV we observe 3443 candidate di-photon events in the sample requiring ≥ 1 jet in the event, while our QCD background estimate in this same region predicts $3636 \pm 79\,(\mathrm{stat.}) \pm 583\,(\mathrm{syst.})$. The estimated EWK background is determined with the ee and $e\gamma$ samples as described above and is calculated to be much smaller than the QCD background. Other backgrounds such as $Z\gamma\gamma \to \nu\nu\gamma\gamma$, $W\gamma\gamma \to \ell\nu\gamma\gamma$, $t\bar{t}\gamma\gamma$, or $Z\gamma\gamma$ events where the $Z \to \tau\tau$ is followed by a τ decay such as $\tau \to \pi\nu$ or $\tau \to e(\mu)\nu\nu$ have been found to be negligible.

The $E_{\mathrm{T}}^{\mathrm{miss}}$ distribution in the $\gamma\gamma$ sample requiring ≥ 1 jet in the event is represented in Fig. 1 as points with errors bars. The green shaded area shows the estimated amount of the EWK background. We assume that events with $E_{\mathrm{T}}^{\mathrm{miss}} \leq 20$ GeV have negligible SUSY signal contribution, and scale the $E_{\mathrm{T}}^{\mathrm{miss}}$ distributions of the average QCD prediction so that the integral of the distribution below 20 GeV matches that in the $\gamma\gamma$ sample minus the estimated EWK contribution. The red hatched areas indicate the total background uncertainties.

Following the previous iteration of this analysis [18], Table 2 summarizes the observed number of $\gamma\gamma$ events with $E_{\mathrm{T}}^{\mathrm{miss}} \geq 100$ GeV and the expected backgrounds with the statistical uncertainty and errors due to re-weighting and normalization shown separately. We observe

Table 2: The number of events with $E_{\mathrm{T}}^{\mathrm{miss}} \geq 100$ GeV from $\gamma\gamma$, ff, and $Z \to ee$ as well as the total number of background events with $E_{\mathrm{T}}^{\mathrm{miss}} \geq 100$ GeV using the ff data. We also show the contributions to the errors due to the re-weighting technique and normalization.

Type	Events	scal. error	norm. error
$\gamma\gamma$ candidates	11		
ff QCD background	10.1 ± 4.2	± 0.3	± 0.03
ee QCD background	14.7 ± 3.1	± 0.1	± 0.03
EWK background	2.9 ± 1.0	± 0.0	± 0.9
Total background (ff)	13.0 ± 4.3		

11 events with $E_{\mathrm{T}}^{\mathrm{miss}} \geq 100$ GeV while the total background expectation is calculated to be $13.0 \pm 4.3\,(\mathrm{stat.}) \pm 4.6\,(\mathrm{syst.})$ events using the ff sample to determine the QCD background plus the EWK background.

We determine the efficiency for SUSY events to pass our analysis cuts by applying correction factors derived from the data to the MC simulation of the signal. Since there is no large clean sample of photons in the data, we rely on similarities between the detector response to electrons and photons to extract the photon efficiency. We obtain a scale factor to apply to the photon MC efficiencies by making a ratio of electron efficiency from $Z \to ee$ events that pass all photon ID cuts (except for the pixel match in data) and the corresponding electron MC efficiencies. We apply the obtained scale factor $0.994 \pm 0.002\,(\mathrm{stat.}) \pm 0.035\,(\mathrm{syst.})$ to the MC photon efficiencies calculated with MC simulation. Other sources of the larger systematic uncertainties in the signal yield include the error on integrated luminosity (4.5%), pile-up effects on photon idendification (2.5%), PDF uncertainty (4-66%) and renormalization scale (4-28%) uncertainty depending on the SUSY signal masses.

Using this measurement and the acceptance times efficiency for the SUSY GGM MC and employing a $\mathrm{CL_S}$ limit-setting method [30], we determine upper limits for GGM SUSY production. In order to maintain a good signal efficiency, the final signal region for the calculation of exclusion limits is defined with a relatively loose selection criteria requiring $E_{\mathrm{T}}^{\mathrm{miss}} \geq 50$ GeV. To still achieve a good sensitivity over a wide range of $E_{\mathrm{T}}^{\mathrm{miss}}$, the limits are calculated in six distinct bins with the following $E_{\mathrm{T}}^{\mathrm{miss}}$ ranges given in GeV: [50,60), [60,80), [80,100), [100,140), [140,180) and [180,∞) and the multi-channel counting experiments are combined into a single limit. We use a log-normal model to incorporate uncertainties on the total background rate, integrated luminosity, and total acceptance times efficiency. The observed 95% C.L. cross-section upper limits vary between 0.002 and 0.012 pb depending on SUSY masses with a typical acceptance of $\sim 30\%$ for $E_{\mathrm{T}}^{\mathrm{miss}} > 50$ GeV and are shown at the top of Fig. 2 for squark and gluino masses between 400 and 2000 GeV for a bino-like neutralino of 375 GeV where the value of 375 GeV was chosen to facilitate comparison with previous results [18].

Since the physical neutralinos and charginos are an admixture of gaugino eigenstates, we have studied two different models of gaugino mixing: one in which the bino mass scale is much lighter than the wino mass scale, and one in which the converse is true. In the former case, the lightest neutralino is always produced at the LHC via the decays of squarks and gluinos, and decays to a Z boson plus a gravitino or a photon plus a gravitino. The lightest chargino is too heavy to play a role. Conversely, in the latter case, both the lightest neutralino and the lightest chargino are produced via squark and gluino decay. The chargino decays to a W boson plus a gravitino. Since, in the latter case, there are more final states available with zero photons, the acceptance for this scenario relative to the total SUSY production rate is significantly lower for

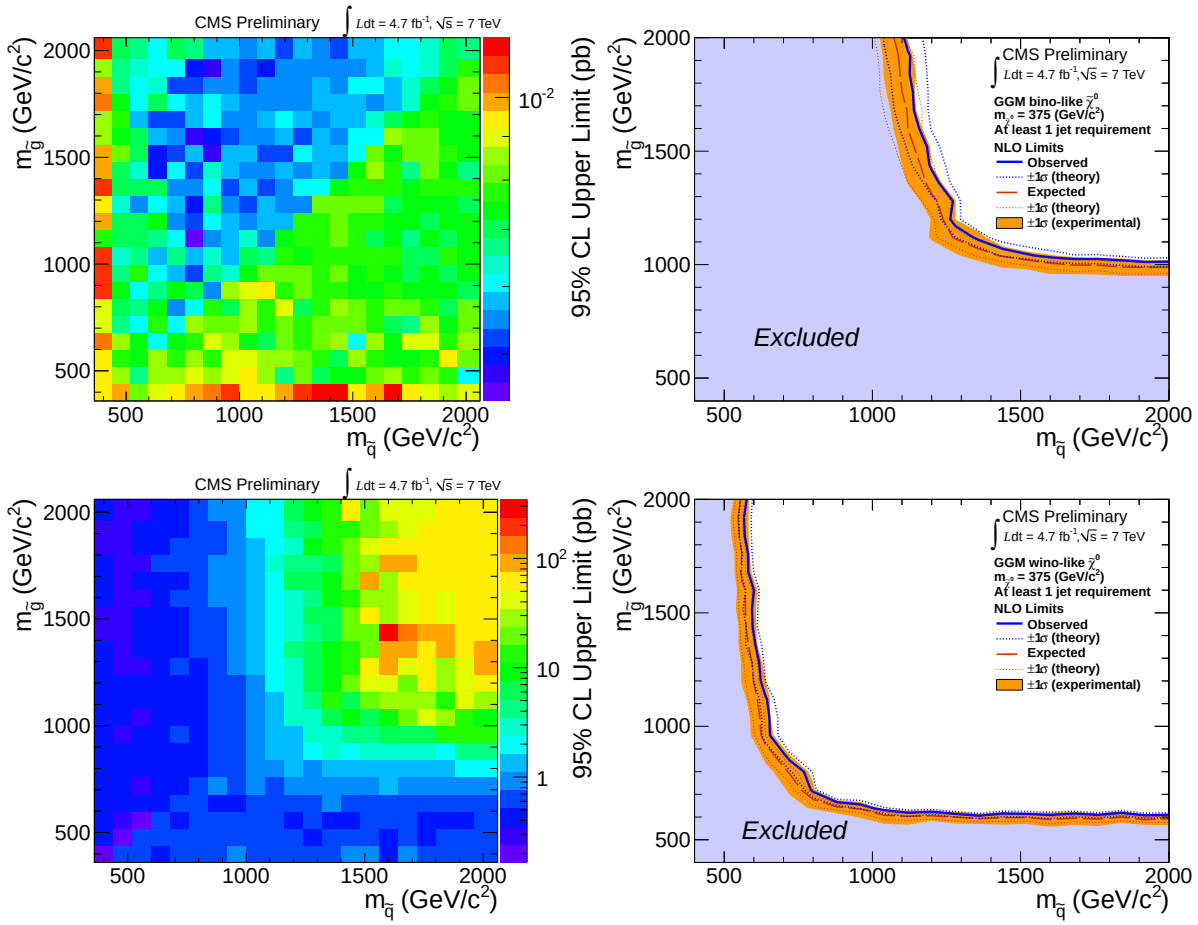

Figure 2: 95% C.L. upper limits on the signal cross section (left) and corresponding exclusion contours (right) in gluino-squark mass space for bino- (top) and wino-like (bottom) neutralino for the di-photon analysis. The shaded uncertainty band around the exclusion contours correspond to the NLO renormalization and PDF uncertainties of the signal cross section.

a given single or di-photon selection. The corresponding limits for a wino-like neutralino are at the bottom of Fig. 2. In the wino-like case the acceptance drops to $\sim 1\%$, leading to an upper limit cross section of ~ 0.01 pb.

As further interpretation of the di-photon result, Figure 3 shows 95% C.L. upper limits on the signal cross section (left) and corresponding exclusion contours (right) for a bino-like neutralino in the plane of gluino versus neutralino mass where the squark mass is fixed at 2.5 TeV/c^2 for this comparison.

5 Single Photon Analysis

The single-photon analysis is based on a trigger requiring the presence of one photon with $E_T > 70$ GeV and the scalar sum (H_T) of the transverse energies of all jets with in the event with $p_T > 40$ GeV and $|\eta| < 3.0$ to be greater than 200-400 GeV. A slight inefficiency of this trigger in a short time period restricts the single photon analysis to an integrated luminosity of 4.3 fb^{-1}. The offline analysis requires $H_T \geq 450$ GeV for the H_T trigger to become fully efficient, and requires at least one tight photon with $E_T > 80$ GeV within $|\eta| < 1.4$. In addition, we require ≥ 2 jets with $p_T \geq 30$ GeV and $|\eta| \leq 2.6$.

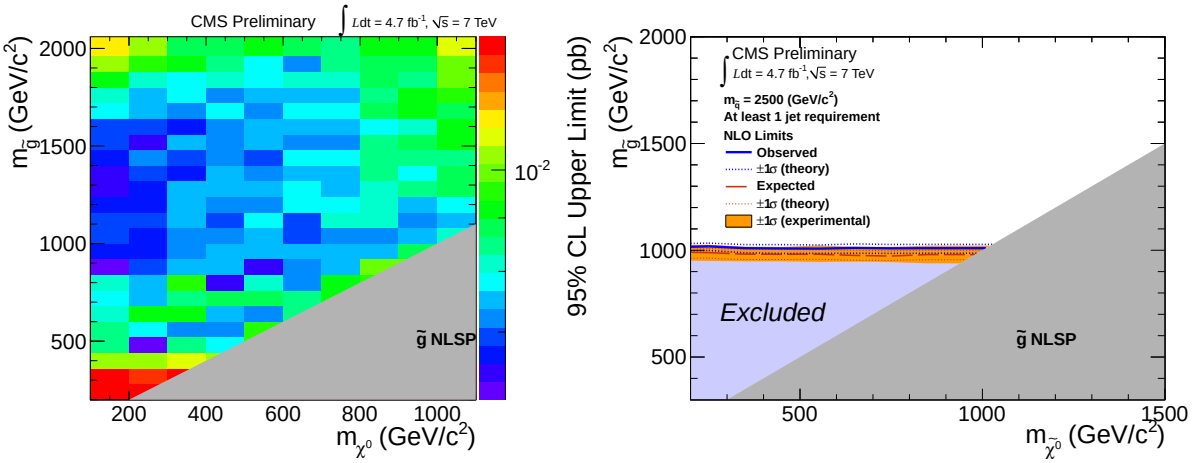

Figure 3: 95% C.L. upper limits on the signal cross section (left) and corresponding exclusion contours (right) for a bino-like neutralino in the plane of gluino versus neutralino mass.

The QCD background in the single-photon analysis is a composition of direct photon-jet production and of QCD multijet production, where one jet is misidentified as a photon. The shape of the $E_{\mathrm{T}}^{\mathrm{miss}}$ distribution, including the non-Gaussian tails, is similar for both background contributions, as the event topology is very similar between the two. Therefore, these two QCD contributions are estimated together from the same data control sample. The control sample is selected by applying the same signal selection requirements, except that the photon candidate is required to fail the tight selection criteria but satisfy a loose isolation requirement. We refer to such photon candidates as γ_{jet}, whose identification is by definition orthogonal to the photon ID criteria in the signal selection. The control sample has to be weighted, to correct for the different p_{T} spectra of γ_{jet} and tight photon objects in the control and signal samples, respectively. The weights are determined in a signal-depleted region with $E_{\mathrm{T}}^{\mathrm{miss}} < 100$ GeV and the weight vs. photon candidate E_{T} is taken from a histogram in bins of p_{T}.

The strategy to model the electroweak background contribution, which is much smaller than the QCD background, is similar to that in the di-photon analysis, as described above. The dominant contributions are from $\mathrm{t\bar{t}}$ production or events with W or Z bosons with one or more neutrinos in the final state. Additional backgrounds can occur due to initial state radiation (ISR) and final state radiation (FSR) of photons. ISR and FSR in events with electrons in the final state are already covered by the electroweak background prediction from data and the remaining contributions from SM process mainly from W, Z and $t\bar{t}$ events are very small and directly taken from Monte Carlo simulation with a conservative systematic uncertainty of 100%. These backgrounds are summarized in Table 3.

The combined background prediction, the observed data and two GGM benchmark signal samples, one excluded and one not excluded, are shown in Fig. 4. The expected and observed event yields are summarized in Table 3. No excess beyond standard model predictions is observed.

The final signal region for the calculation of exclusion limits is defined with a relatively loose selection criteria requiring $E_{\mathrm{T}}^{\mathrm{miss}} \geq 100$ GeV. To still achieve a good sensitivity, the limits are calculated in six distinct bins with the following $E_{\mathrm{T}}^{\mathrm{miss}}$ ranges in GeV: [100,120), [120,160), [160,200), [200,270), [270,350) and [350,∞). In the same way as described for the di-photon analysis above, the multi-channel counting experiments are combined into a single limit. We again use the $\mathrm{CL_S}$ method to determine 95% confidence level (C.L.) upper limits for the squark versus gluino mass plane from 400 to 2000 GeV in squark and gluino mass with the neutralino

Table 3: Resulting event yields for the ≥1 photon + ≥2 jet selection for three different signal regions ($E_T^{miss} > 100/200/350$ GeV). The FSR/ISR statistical errors are due to limited MC statistics.

	$E_T^{miss} \geq 100$ GeV			$E_T^{miss} \geq 200$ GeV			$E_T^{miss} \geq 350$ GeV		
$\geq 1\gamma, \geq 2$ jets		(stat.)	(syst.)		(stat.)	(syst.)		(stat.)	(syst.)
QCD (from data)	607.7	±46.7	±54.0	90.7	±16.4	±9.9	6.8	±4.1	±0.8
$e \to \gamma$ (from data)	17.2	±0.3	±7.2	3.5	±0.2	±1.5	0.4	±0.01	±0.2
FSR/ISR(W, Z)	27.6	±3.2	±27.6	10.4	±2.0	±10.4	1.6	±0.8	±1.6
FSR/ISR$(t\bar{t})$	3.8	±0.9	±3.8	0.8	±0.4	±0.8	< 0.01	< 0.01	< 0.01
total SM estimate	656.4	±46.9	±92.7	105.5	±16.5	±22.6	8.7	±4.2	±2.5
Data	615			63			4		

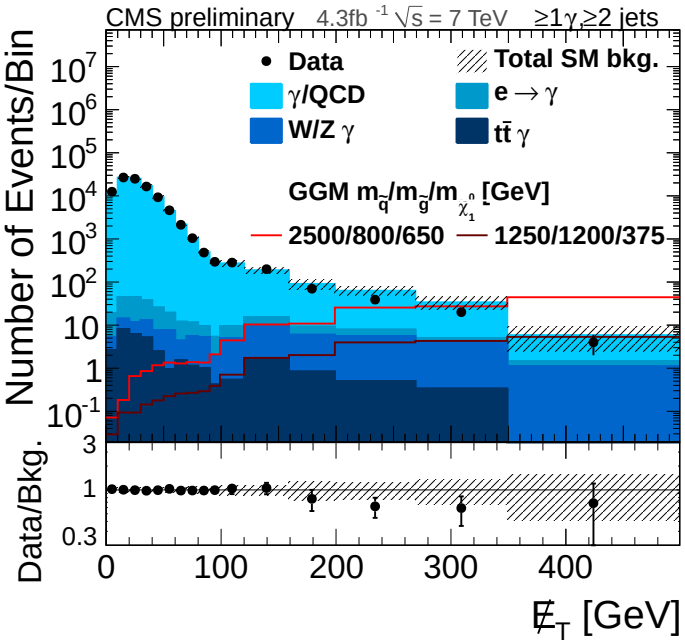

Figure 4: Total standard model background prediction compared to the number of single-photon events, including two GGM benchmark signal benchmark points as examples where masses ($m_{\tilde{q}}/m_{\tilde{g}}/m_{\tilde{\chi}_1^0}$) are given in GeV.

mass set again at 375 GeV to facilitate comparison with previous results [18].

A possible contamination of signal in the background sample used for the background estimation has been studied and is considered in the limit calculation. For this purpose the expected amount of SUSY GGM events in the background estimation has been subtracted from the number of observed signal events, lowering the acceptance times efficiency by a few percent for each point. The resulting limits, after subtraction of the signal contamination, are shown in Fig. 5. For the bino-like scenario the resulting upper limit cross section is of order 0.01 pb with a typical acceptance of ∼ 77% for $E_T^{miss} > 100$ GeV. For the wino like scenario the acceptance drops to ∼ 7%, leading to an upper limit cross section of ∼ 0.08 pb.

As further interpretation of the single photon result, Figure 6 shows 95% C.L. upper limits

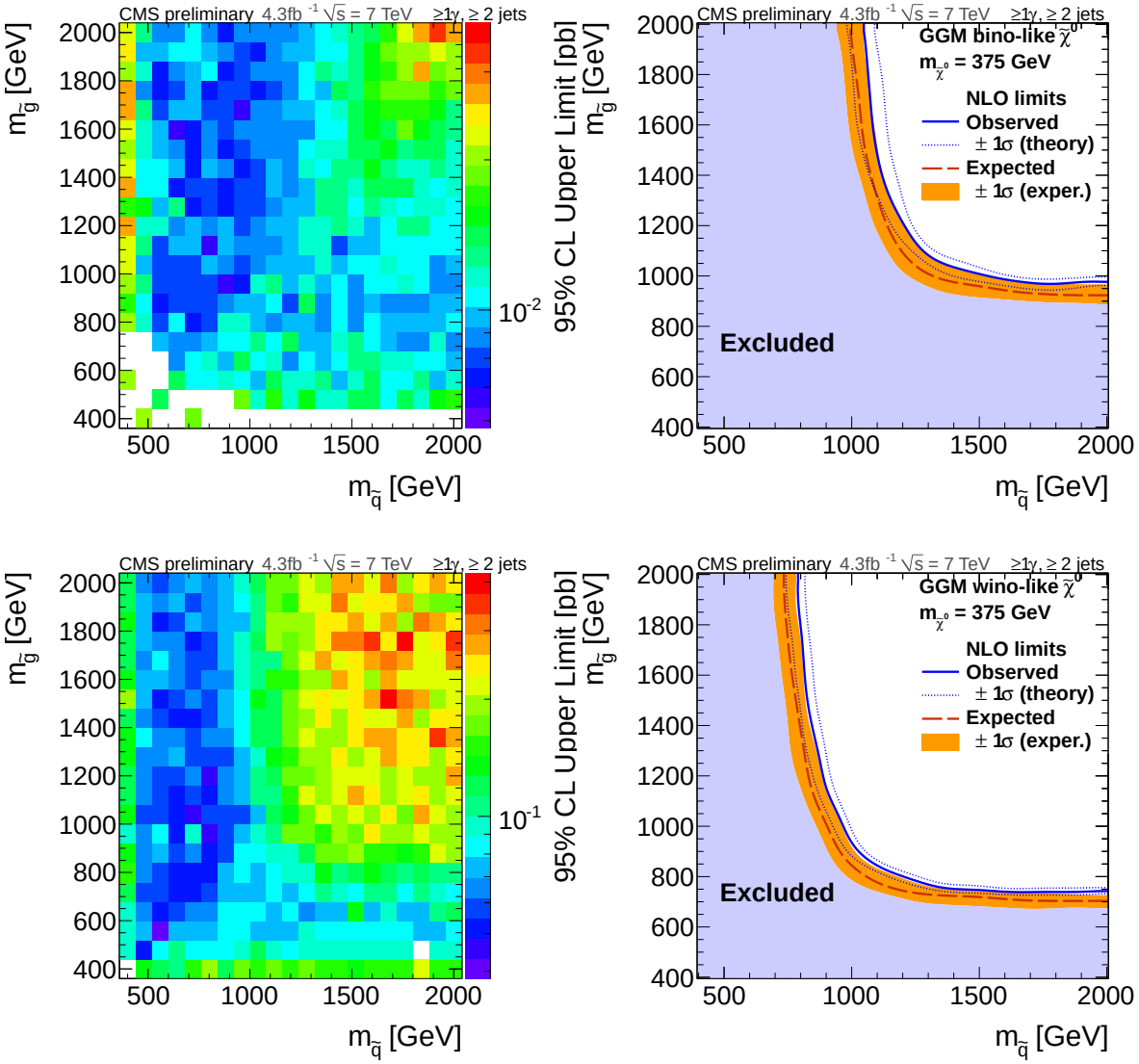

Figure 5: 95% C.L. upper limits on the signal cross section (left) and corresponding exclusion contours (right) in gluino-squark mass space for bino- (top) and wino-like (bottom) neutralino for the single photon analysis. The shaded uncertainty band around the exclusion contours correspond to the NLO renormalization and PDF uncertainties of the signal cross section.

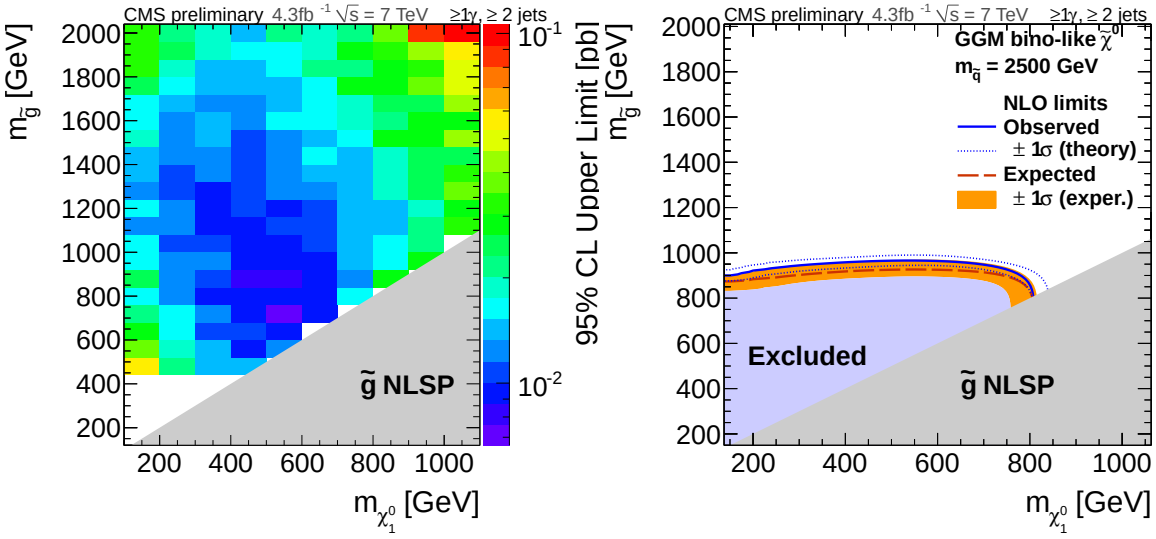

Figure 6: 95% C.L. upper limits on the signal cross section (left) and corresponding exclusion contours (right) for a bino-like neutralino in the plane of gluino versus neutralino mass.

on the signal cross section (left) and corresponding exclusion contours (right) for a bino-like neutralino in the plane of gluino versus neutralino mass.

6 Search for Universal Extra Dimensions

Di-photon final states with large $E_{\mathrm{T}}^{\mathrm{miss}}$ similar to those expected from GGM SUSY scenarios are also predicted by the theory of Universal Extra Dimensions (UED). Therefore, the di-photon GGM result can be re-interpreted into a limit for the UED model [31]. UED postulates the existence of additional compactified dimensions where standard model fields are allowed to propagate, and provides several interesting results including gauge coupling unification, supersymmetry breaking, and other phenomena beyond the standard model [31]. As SM particles propagate through the additional dimensions excitations are created. These excitations, known as Kaluza-Klein (KK) towers, can then decay eventually to the lightest Kaluza-Klein particle (LKP), which is the KK photon.

To produce the di-photon final state similar to GGM, it is assumed that the UED space is embedded in an additional space that has N Large Extra Dimensions (LEDs) where only the graviton propagates. Then the LKP is allowed to decay gravitationally, producing a photon and a graviton. As the dominant production method at the LHC is from the strong interaction, KK quark and gluon pairs are produced, cascading down to two LKP decays resulting in the two photon plus jet(s) and $E_{\mathrm{T}}^{\mathrm{miss}}$ final state. Parameters for this model are chosen to match the two previous UED studies, first by D0 at the Tevatron which excluded $1/R < 477$ GeV [32] and most recently by ATLAS which excluded $1/R < 728$ GeV [8].

The cross section upper limit for the production of KK particles, which would indicate the presence of UEDs, can be calculated in the same way as for GGM. The maximum UED productions cross section is computed using the acceptance times efficiency from signal Monte Carlo simulations and the same luminosity, background, and number of observed events as for the GGM calculation. The UED cross sections and the cross section 95% C.L. upper limit are interpolated and their intersection is determined. This intersection is shown in Figure 7. Uncertainties due

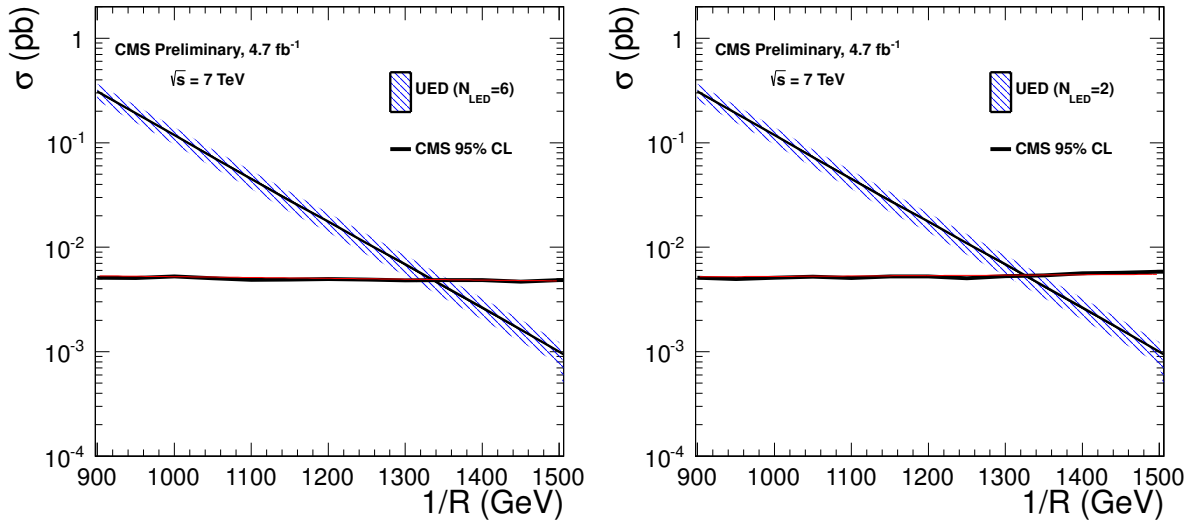

Figure 7: The UED cross section upper limit for 6 (left), and 2 (right) LEDs at the 95% C.L. is compared with UED LO production cross sections. Intersection of the central cross section value implies exclusion of all values of $1/R < 1335\ (1323)$ GeV for 6 (2) LEDs. The shaded region shows uncertainty due to PDFs and renormalization scale.

to PDFs and renormalization scale are shown as the shaded region, while the intersection of the central value implies that all values of $1/R < 1335$ GeV for $N_{\text{LEDs}} = 6$ are excluded. For $N_{\text{LEDs}} = 2$ the exclusion limit is reduced to 1323 GeV.

7 Summary

In summary, we have searched for evidence of GGM SUSY production in di-photon and single-photon events using the $E_{\text{T}}^{\text{miss}}$ spectrum beyond 100 GeV. This search is based on 2011 CMS data comprising 4.7 fb^{-1} of pp collisions at $\sqrt{s} = 7$ TeV. We find no evidence of GGM SUSY production and set upper limits for a range of parameters in that model. For the single and di-photon analyses we have defined 95% C.L. exclusion regions for the production cross sections in the GGM SUSY parameter space of squark and gluino masses of order 0.01 pb (0.1 pb) for the bino- (wino-) like scenarios. We also present exclusion contours for a bino-like neutralino in the plane of gluino versus neutralino mass. Finally, the di-photon analysis is re-interpreted as a search for Universal Extra Dimensions leading to 95% exclusion values of $1/R < 1335$ GeV for $N_{\text{LEDs}} = 6$.

References

[1] P. Fayet, "Mixing Between Gravitational and Weak Interactions Through the Massive Gravitino", *Phys. Lett.* **B70** (1977) 461. doi:10.1016/0370-2693(77)90414-2.

[2] H. Baer, M. Brhlik, C. H. Chen et al., "Signals for the Minimal Gauge-Mediated Supersymmetry Breaking Model at the Fermilab Tevatron Collider", *Phys. Rev.* **D55** (1997) 4463. doi:10.1103/PhysRevD.55.4463.

[3] H. Baer, P. G. Mercadante, X. Tata et al., "Reach of Tevatron Upgrades in Gauge-Mediated Supersymmetry Breaking Models", *Phys. Rev.* **D60** (1999) 055001. doi:10.1103/PhysRevD.60.055001.

[4] S. Dimopoulos, S. Thomas, and J. D. Wells, "Sparticle Spectroscopy and Electroweak Symmetry Breaking with Gauge-Mediated Supersymmetry Breaking", *Nucl. Phys.* **B488** (1997) 39. doi:10.1016/S0550-3213(97)00030-8.

[5] J. R. Ellis, J. L. Lopez, and D. V. Nanopoulos, "Analysis of LEP Constraints on Supersymmetric Models with a Light Gravitino", *Phys. Lett.* **B394** (1997) 354. doi:10.1016/S0370-2693(97)00019-1.

[6] M. Dine, A. Nelson, Y. Nir et al., "New Tools for Low Energy Dynamical Supersymmetry Breaking", *Phys. Rev.* **D53** (1996) 2658. doi:10.1103/PhysRevD.53.2658.

[7] G. F. Giudice and R. Rattazzi, "Gauge-Mediated Supersymmetry Breaking", in *Perspectives on Supersymmetry*, p. 355. World Scientific, Singapore, 1998.

[8] ATLAS Collaboration, "Search for Diphoton Events with Large Missing Transverse Energy with 36 pb^{-1} of 7 TeV Proton-Proton Collision Data with the ATLAS Detector", *Eur. Phys. J.* **C71** (2011) 1744, arXiv:1107.0561. doi:10.1140/epjc/s10052-011-1744-9.

[9] ATLAS Collaboration, "Search for Diphoton Events with Large Missing Transverse Momentum in 1 $fb^{-}1$ of 7 TeV Proton-Proton Collision Data with the ATLAS Detector", arXiv:1111.4116.

[10] CMS Collaboration, "Search for Supersymmetry in pp Collisions at sqrt(s) = 7 TeV in Events with Two Photons and Missing Transverse Energy", *Phys. Rev. Lett.* **106** (2011) 211802. doi:10.1103/PhysRevLett.106.211802.

[11] T. Aaltonen et al., "Search for Supersymmetry with Gauge-Mediated Breaking in Diphoton Events with Missing Transverse Energy at CDF II", *Phys. Rev. Lett.* **104** (2010) 011801. doi:10.1103/PhysRevLett.104.011801.

[12] V. M. Abazov et al., "Search for Diphoton Events with Large Missing Transverse Energy in 6.3 fb^{-1} of $p\bar{p}$ Collisions at $\sqrt{s}$ = 1.96 TeV", *Phys. Rev. Lett.* **105** (2010) 221802. doi:10.1103/PhysRevLett.105.221802.

[13] A. Heister et al., "Search for Gauge Mediated SUSY Breaking Topologies in e^+e^- Collisions at Centre-of-Mass Energies up to 209 GeV", *Eur. Phys. J.* **C25** (2002) 339. doi:10.1007/s10052-002-1005-z.

[14] J. Abdallah et al., "Photon Events with Missing Energy in e^+e^- Collisions at $\sqrt{(}s) = 130$ to 209 GeV", *Eur. Phys. J.* **C38** (2005) 395. doi:10.1140/epjc/s2004-02051-8.

[15] P. Achard et al., "Single- and Multi-Photon Events with Missing Energy in e^+e^- Collisions at LEP", *Phys. Lett.* **B587** (2004) 16. doi:10.1016/j.physletb.2004.01.010.

[16] G. Abbiendi et al., "Search for Gauge-Mediated Supersymmetry Breaking Topologies in e^+e^- Collisions at LEP2", *Eur. Phys. J.* **C46** (2006) 307. doi:10.1140/epjc/s2006-02524-8.

[17] A. Aktas et al., "Search for Light Gravitinos in Events with Photons and Missing Transverse Momentum at HERA", *Phys. Lett.* **B616** (2005) 31. doi:10.1016/j.physletb.2005.04.038.

[18] CMS Collaboration, "Search for Supersymmetry in Events with Photons, Jets and Missing Energy", CMS Physics Analysis Summary CMS-PAS-SUS-11-009, (2011).

[19] LHC New Physics Working Group, "Simplified Models for LHC New Physics Searches", (2010). See http://www.lhcnewphysics.org/photons.

[20] P. Meade, N. Seiberg, and D. Shih, "General Gauge Mediation", *Prog. Theor. Phys. Suppl.* **177** (2009) 143. doi:10.1143/PTPS.177.143.

[21] M. Buican, P. Meade, N. Seiberg et al., "Exploring General Gauge Mediation", *JHEP* **0903** (2009) 016. doi:10.1088/1126-6708/2009/03/016.

[22] CMS Collaboration, "Search for New Physics with Long-Lived Particles Decaying to Photons and Missing Energy", CMS Physics Analysis Summary CMS-PAS-EXO-11-067, (2011).

[23] G. R. Farrar and P. Fayet, "Phenomenology of the Production, Decay, and Detection of New Hadronic States Associated with Supersymmetry", *Phys. Lett.* **B76** (1978) 575. doi:10.1016/0370-2693(78)90858-4.

[24] CMS Collaboration, "The CMS experiment at the CERN LHC", *JINST* **03** (2008) S08004. doi:10.1088/1748-0221/3/08/S08004.

[25] P. Adzic et al., "Energy resolution of the barrel of the CMS electromagnetic calorimeter", *JINST* **2** (2007) P04004. doi:10.1088/1748-0221/2/04/P04004.

[26] CMS Collaboration, "Particle–Flow Event Reconstruction in CMS and Performance for Jets, Taus, and $E_{\mathrm{T}}^{\mathrm{miss}}$", *CMS Physics Analysis Summary* **CMS-PAS-PFT-09-001** (2009).

[27] T. Sjostrand, S. Mrenna, and P. Z. Skands, "PYTHIA 6.4 Physics and Manual", *JHEP* **0605** (2006) 026, arXiv:hep-ph/0603175. doi:10.1088/1126-6708/2006/05/026.

[28] W. Beenakker, R. Höpker, M. Spira et al., "Squark and Gluino Production at Hadron Colliders", *Nucl. Phys.* **B492** (1997) 51. doi:10.1016/S0550-3213(97)80084-9.

[29] GEANT4 Collaboration, "GEANT4: A Simulation toolkit", *Nucl.Instrum.Meth.* **A506** (2003) 250–303. doi:10.1016/S0168-9002(03)01368-8.

[30] Particle Data Group Collaboration, "Review of particle physics", *J. Phys.* **G37** (2010) 075021. doi:10.1088/0954-3899/37/7A/075021.

[31] T. Appelquist, H.-C. Cheng, and B. A. Dobrescu, "Bounds on universal extra dimensions", *Phys. Rev.* **D64** (2001) 035002, arXiv:hep-ph/0012100. doi:10.1103/PhysRevD.64.035002.

[32] D0 Collaboration, "Search for diphoton events with large missing transverse energy in 6.3 fb^{-1} of $p\bar{p}$ collisions at $\sqrt{s} = 1.96$ TeV", *Phys. Rev. Lett.* **105** (2010) 221802, arXiv:1008.2133. doi:10.1103/PhysRevLett.105.221802.